Review

Not peer-reviewed version

Improving Nuclear Magnetic Dipole Moments: Gas Phase NMR Spectroscopy Research

Włodzimierz Makulski *

Posted Date: 3 December 2025

doi: 10.20944/preprints202512.0399.v1

Keywords: NMR spectra; nuclear magnetic dipole moments; diamagnetic corrections; gas phase

doi:10.20944/preprints202512.0399.v1

Review

Improving Nuclear Magnetic Dipole Moments: Gas Phase NMR Spectroscopy Research

Włodzimierz Makulski

Laboratory of NMR Spectroscopy, Faculty of Chemistry, University of Warsaw, Pasteura 1, 02-093 Warszawa, Poland; wmakul@chem.uw.edu.pl; Tel.: +48 (22) 5526370

Abstract

High-resolution NMR spectroscopy is the leading method for determining nuclear magnetic moments. It is designed to measure stable nuclei that can be investigated in macroscopic samples. In this work, we discuss the progress in research into light nuclei from the first three periods of the Periodic Table and several selected heavy nuclides. New ^{1}H and ^{3}He nuclei using the Penning trap method are also considered. Both nuclei can be used as references in gaseous mixtures. Gas-phase NMR spectroscopy enables precise measurements of the frequencies and shielding constants of isolated single molecules. They can be used to determine new, accurate nuclear magnetic moments of nuclides in stable, gaseous substances. Particular attention is paid to the importance of diamagnetic corrections for obtaining accurate results. Finding precise diamagnetic corrections - shielding factors, even in the case of light nuclei in molecules, is a big challenge. Up to now, nuclear moments have been obtained primarily from experimental results. The theoretical approach is mostly unable to predict these values accurately. Some remarks are also made on pure theoretical treatments of nuclear moments.

Keywords: NMR spectra; nuclear magnetic dipole moments; diamagnetic corrections; gas phase.

---

1. Introduction

Nuclear magnetic moments are related to a nucleus with nuclear spin, and they are expressed as a vector sum of the magnetic moments of the nucleons inside it. This is a valuable physical variable (μ), and it can be used in tests of different calculation theories. These are "ab initio", semiempirical, or density functional theory calculations. Unfortunately, progress in theoretical computations is still limited to light nuclei, and nuclear magnetic moments are generally treated as experimental quantities. Tables of Nuclear Magnetic Dipole Moments have been published periodically by N.J. Stone for several years. One of the most effective methods for establishing these values is NMR spectroscopy. In this technique, the most critical information is the specific radiofrequency at the peak response in the absorption spectrum. This frequency is proportional to the static B_0 field, the nuclear magnetic moment of the nucleus observed, and shielding effects. Besides the frequencies being observed (ν), a crucial role in the procedure for measuring the nuclear magnetic moments is attributed to knowledge of minor but valuable corrections for shielding effects (σ), previously known as diamagnetic effects. This paper describes recent developments in the determination of nuclear magnetic moments using NMR spectroscopy. The nuclides we are interested in are shown in Figure 1 below.

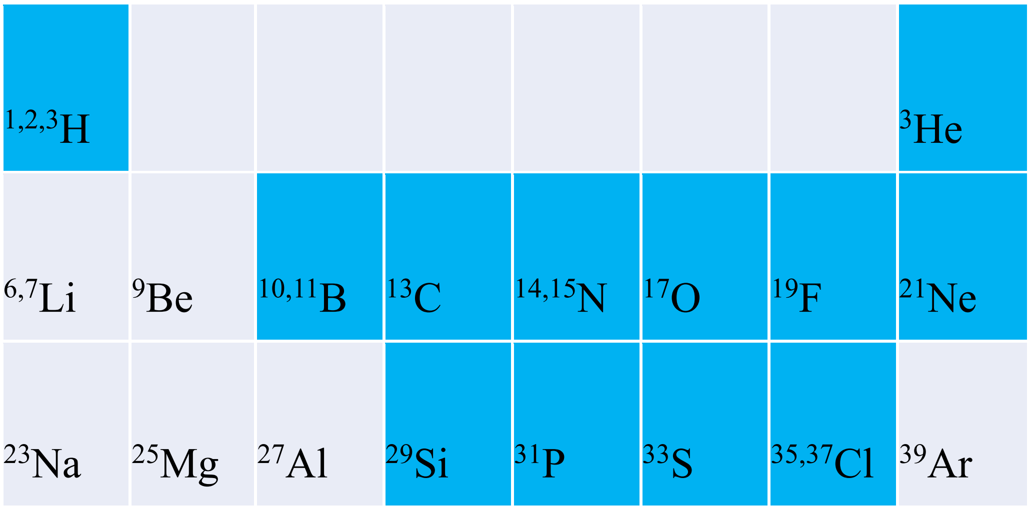

^{1,2,3}H							^{3}He
^{6,7}Li	^{9}Be	^{10,11}B	^{13}C	^{14,15}N	^{17}O	^{19}F	^{21}Ne
^{23}Na	^{25}Mg	^{27}Al	^{29}Si	^{31}P	^{33}S	^{35,37}Cl	^{39}Ar

Figure 1. NMR active nuclei from the first three rows of the Periodic Table.

In the Laboratory of NMR Spectroscopy at the Department of Chemistry at Warsaw University, we have performed several studies in this field in the gaseous state, where diamagnetic corrections and appropriate frequencies can be incorporated throughout the procedure. Gas-phase physical properties can be written as linear functions of the pressure/density of the prepared samples. The linear regression method is used for analytical solving of linear dependencies. The line of the best fit can give extrapolated NMR parameters for a single "isolated" molecule. The paper covers the experimental details and final results for nuclides from the first three rows of the Periodic Table of Elements, obtained from gaseous experiments, all of which are highly precise and accurate.

2. Methodology

2.1. NMR Method of μ(X) Measurements

To obtain an NMR signal, the conditions require inducing flipping between different nuclear magnetic orientations in the static magnetic field B_0. In spectroscopy machines, the B_0 field is produced by superconducting magnets, with fields ranging from 1T to ~22T (1T = Tesla). The appropriate electromagnetic waves are in the radio frequency (RF) region from 100 MHz to ~1000 MHz. To absorb a portion of energy in the NMR regime, the simple relations known as Larmor equations need to be fulfilled:

$$h\nu_Y = \Delta\mu_Y^z(1-\sigma_Y)B_z \tag{1}$$

$$h\nu_X = \Delta\mu_X^z(1-\sigma_X)B_z, \tag{2}$$

where B_z represents the z component of the firm, stable, and homogeneous magnetic field B_0.
The precession (rotation) of the nuclear magnetic moments (NMM) occurs around the z-axis of the magnetic field (for two different nuclei: ν_X and ν_Y) at a constant rate ω_L, which can be observed in the NMR spectrometer as a radio resonance frequency, where σ_X and σ_Y are the absolute shielding constants. The conventional relationship between two nuclear magnetic moments and two observed frequencies (ν_X, ν_Y) measured in the given sample in the same magnetic field B_0 can be formulated as [1]:

$$\Delta\mu_Y^z = \frac{\nu_Y}{\nu_X}\cdot\frac{(1-\sigma_X)}{(1-\sigma_Y)}\cdot\frac{I_Y}{I_X}\cdot\Delta\mu_X^z \tag{3}$$

Where μ_X and μ_Y are two different magnetic moments, ν_X and ν_Y are NMR frequencies from the spectra, and σ_X and σ_Y are shielding constants often called diamagnetic corrections. Measurements of nuclear magnetic dipole moments using NMR spectroscopy are exact and accurate. These measurements are very well suited for studies of stable isotopes and those for which decay is slow (see, for example, $^3H(T)$). Finally, we can consider Eq.(3) converted in the form:

$$\sigma_X = 1 - \frac{\nu_X}{\nu_Y} \cdot \frac{\Delta\mu_X}{\Delta\mu_Y} \cdot \frac{I_X}{I_Y} \cdot (1 - \sigma_Y) \tag{4}$$

This will be used to check the consistency of the new shielding results and nuclear magnetic moments. It is possible to use other pairs of nuclei than those applied in Eq. (3). In this case, experiments with the addition of helium-3 gas are beneficial.

2.2. Gas Phase NMR Measurements

The most well-known extension of the gas property in powers of density is the so-called "virial expansion". The dependence of density and pressure for any molecular property in a pure gas can be expressed in this straightforward manner. Several physical properties of gases can be easily understood using the general virial theorem [2]. In our case, the more important property – the nuclear magnetic shielding of a given nucleus in a pure gas $\sigma(\varrho, T)$ can be described as a virial expansion in the density function (ϱ) at a specific temperature (T), as shown here [2]:

$$\sigma(\varrho,T) = \sigma_0 + \sigma_1(T)\varrho + \sigma_2(T)\varrho^2 + \sigma_3(T)\varrho^3 + \dots \tag{5}$$

Where σ_0 is the shielding constant of the nucleus in the "isolated" atom or molecule, and σ_1, σ_2, and σ_3 are virial coefficients arising from two, three, or more-body collisions. At low pressures (density below ~1.64 mol/L at 297 K), the dependences are strictly linear because only the first two coefficients are essential, in this manner:

$$\sigma(\varrho,T) = \sigma_0 + \sigma_1(T)\varrho \tag{6}$$

Similar equations can be used when exploring mixtures of gaseous substances. These systems can be studied as binary mixtures of a gaseous substance A containing the nucleus X, whose shielding $\sigma(X)$ is measured, and gas B, the solvent. Equation (1) can be written as:

$$\sigma(X) = \sigma_0(X) + \sigma_{AA}(X)\varrho_A + \sigma_{AB}(X)\varrho_B + \dots \tag{7}$$

Where ϱ_A and ϱ_B are the densities of substances A and B, the coefficients $\sigma_{AA}(X)$ and $\sigma_{AB}(X)$ contain the bulk susceptibility corrections ($(\sigma_A)_b$ and $(\sigma_B)_b$) and the terms involving intermolecular interactions during the A–A and A–B collisions ($\sigma_{A\text{-}A}(X)$ and $\sigma_{A\text{-}B}(X)$). Again, if the concentration of substance A under investigation is sufficiently low (usually < 1%), the $\sigma_{AA}(X)$ can be entirely omitted, and the final equation is:

$$\sigma(X) = \sigma_0(X) + \sigma_{AB}(X)\varrho_B \tag{8}$$

Equation (6) was used for pure simple gases such as CH_4, SiH_4, and PH_3. Sometimes the additional ingredients were maintained by small amounts of gaseous ^3He. In this case, equation (7) is valid because the amount of helium is small. Contributions to σ_1 or σ_{AB} include the Van der Waals field, the electric field, and the molecular anisotropy of neighboring molecules, as well as the bulk susceptibility. The bulk susceptibility ($4\pi\chi_M/3$ in B ∥ external field) can generally be removed from σ_1 or σ_{AB}, so that only the proper intermolecular effects are present. Each σ_1 parameter is described by a complex function of the intermolecular separation and orientation between two interacting molecules (an intermolecular shielding surface). Ab initio methods can calculate this function, but the appropriate procedure is computationally intensive and, to date, has been obtained only for the simplest molecular systems.

2.3. State-Of-The-Art Quantum Mechanical Computations

Gas-phase NMR measurements are usually straightforward and can yield precise frequency measurements when relaxation times are sufficiently long and the spectral resolution is sufficiently high. On the other hand, diamagnetic corrections (shielding constants) are more demanding and need the application of advanced theoretical studies. Nuclear shielding in molecules is, in principle, the function of their electronic structure. Usually, a large number of electrons increases the shielding effect; however, several deshielding effects have also been observed in diamagnetic molecules [3]. Gas-phase experiments allow us to eliminate all intermolecular interactions by extrapolating shielding measurements to the zero-pressure limit. In this context, the experiment is associated with a significant part of quantum chemical calculations, designated to the so-called "isolated" single molecules. More popular methods include perturbative treatments. In a perturbative theoretical approach, iterative corrections yield approximate solutions [4]. The gauge-including atomic orbitals (GIAO) approach is employed chiefly here, incorporating magnetic-field-dependent gauge factors into the atomic basis sets. Several approximate perturbation theories with specific variants are used: the HF (Hartree-Fock), MCSCF (Multi-Configuration Self-Consistent-Field), the CC (Coupled Cluster), such as CCS, CC2, CCSD, CCSDT, etc., and the MP (Möller-Plesset) model up to FCI (Full Configuration Interaction). In larger molecules, the same specific methods were used: DFT (Density Functional Theory) or the ONIOM method, with great success [3]. NMR spectral parameters are first computed for the molecule's equilibrium geometry, which can be experimental or fully optimised to minimise electron repulsion forces. These shielding values $\sigma_e(X)$ are then corrected for vibrations and rotations, e.g., applying the zero-point vibration correction $\sigma(X)_{ZPV}$ and averaging over the Boltzmann distribution up to room temperature $\sigma(X)_T$ (usually at 300K). Sometimes, using gas-phase NMR data, one can separate these corrections by studying isotope effects and comparing them with quantum-chemical computations (*e.g.*, for the H_2O molecule [5]). Three factors influence calculations of NMR parameters: the size of the basis set, electron correlation, and relativistic effects. Electron correlation effects were implemented in the primary methods mentioned above. Even for light nuclei, it is essential to account for relativistic corrections. For example, within the so-called four-component relativistic framework, the absolute shielding of the isolated NH_3 molecule was established [6]. For the BF_3 molecule, the shielding constant was obtained as the sum of a nonrelativistic electron-correlated contribution and a relativistic correction computed at a lower level of theory [7]. The spin-rotation and nuclear magnetic shielding constants are analysed for both nuclei in the HCl molecule [8]. Nonrelativistic ab initio calculations at the CCSD(T) level of theory show that relativistic effects are essential to obtain spin-rotation constants consistent with accurate experimental data. For small molecules, experimentally determined nuclear magnetic shielding should be consistent with that computed using the more sophisticated methods.

2.4. Absolute Shielding Scales

Standard NMR spectra make it possible to measure the chemical shifts (δ), values expressed in ppm units against the reference, which is the liquid sample taken arbitrarily during the NMR development. Nevertheless, the more fundamental measure of electron screening effects is nuclear magnetic shielding (σ). The absolute shielding scale is a measure of the local magnetic field at a nucleus, influenced by the nearby electron clouds. It consists of several results for a series of molecules with well-known shielding constants at room temperature (preferably 300K) and one liquid reference substance. The absolute shielding scales utilise the magnetic shielding of at least one simple compound, for which the shielding constant is well documented and widely accepted [3]. For example, ^{1}H [9] and ^{13}C [10] NMR shielding is well established for many small "isolated" molecules, and the CH_4 molecule is a primary reference. For other nuclei, new, usually complicated and bothersome theoretical studies are necessary, at least for a simple molecule considered as a reference. They should distinguish between intramolecular and intermolecular effects on the shielding tensor, depending on the external and induced fields at a given nucleus. They can often be compared with experimental results [11]. The liquid reference substance, e.g., *TMS* (tetramethylsilane), can be used in ^{1}H, ^{13}C, and ^{29}Si resonance studies to evaluate results obtained in both gaseous and liquid states. For the determination of the nuclear shielding in the molecule on which the scale is based, it is possible to use different measurable quantities: spin precession frequencies, spin rotation constants, and/or nuclear relaxation times [3]. Gas-phase experiments are preferred because they allow the removal of strong intermolecular interactions that are always present in condensed phases. They are omitted entirely when gas-phase results are extrapolated to the zero-pressure limit. Using these methods, absolute shielding scales for ^{1}H, ^{13}C, ^{15}N, and ^{29}Si, as well as for other nuclei, were established. An alternative procedure for determining absolute shielding scales is based on the Ramsey–Flygare relationship [10], which, for heavy nuclei, requires relativistic corrections. The Ramsey–Flygare relationship allows one to determine nuclear shielding from the spin-rotation constant. Recent developments in absolute shielding scales for NMR spectroscopy and relativistic effects on nuclear magnetic shielding are discussed in Refs. [12,13].

3. Results

The previously studied gaseous systems are listed in Table 1.

Table 1. Gas-phase NMR measurement systems for nuclear magnetic moments (NMM) have been developed over the past 20 years.

NMR spectra	NMM. transfer	Molecules
^{1}H and $^{2}H(D)$	$^{1}H \rightarrow {}^{2}H(D)$	HD
^{1}H and $^{3}H(T)$	$^{1}H \rightarrow {}^{3}H(T)$	HT
^{19}F and ^{10}B	$^{19}F \rightarrow {}^{10}B$	BF_3
^{19}F and ^{3}He	$^{3}He \rightarrow {}^{10}B$	$BF_3/{}^{3}He$
^{19}F and ^{11}B	$^{19}F \rightarrow {}^{11}B$	BF_3
^{19}F and ^{3}He	$^{3}He \rightarrow {}^{11}B$	$BF_3/{}^{3}He$
^{1}H and ^{13}C	$^{1}H \rightarrow {}^{13}C$	$^{13}CH_4$
^{3}He and ^{13}C	$^{1}H \rightarrow {}^{13}C$	$^{13}CH_4/{}^{3}He$
^{1}H and ^{14}N	$^{1}H \rightarrow {}^{14}N$	NH_3
^{3}He and ^{14}N	$^{3}He \rightarrow {}^{14}N$	$NH_3/{}^{3}He$
^{1}H and ^{15}N	$^{1}H \rightarrow {}^{15}N$	NH_3
^{3}He and ^{15}N	$^{3}He \rightarrow {}^{15}N$	$NH_3/{}^{3}He$
^{1}H and ^{17}O	$^{1}H \rightarrow {}^{17}O$	H_2O
^{1}H and ^{19}F	$^{1}H \rightarrow {}^{19}F$	CH_3F
^{1}H and ^{29}Si	$^{1}H \rightarrow {}^{29}Si$	SiH_4
^{1}H and ^{31}P	$^{1}H \rightarrow {}^{31}P$	PH_3
^{3}He and ^{31}P	$^{3}He \rightarrow {}^{31}P$	$PH_3/{}^{3}He$
^{3}He and ^{33}S	$^{3}He \rightarrow {}^{33}S$	$SF_6/{}^{3}He$
^{1}H and $^{35/37}Cl$	$^{1}H \rightarrow {}^{35/37}Cl$	HCl
^{3}He and $^{35/37}Cl$	$^{3}He \rightarrow {}^{35/37}Cl$	$HCl/{}^{3}He$

Experimental values of nuclear moments for light nuclei, from the first rows of the Periodic Table, can be found in Table 2. They belong to particular nuclei: hydrogen isotopes $^{1/2/3}H$, ^{3}He, ^{13}C, ^{14}N, ^{15}N, ^{17}O, ^{19}F, ^{21}Ne, ^{29}Si, ^{31}P, ^{33}S and $^{35/37}Cl$. All values are expressed in the units of the nuclear magneton, i.e., $\mu_N = 5.0507837393(16)\times10^{-27}$ JT^{-1}. The nuclear magneton is a physical constant calculated as $\mu_N = e\hbar/2cm_p$ where p refers to the proton. The previously published results are in the third column of the table and marked as cited from Ref.[14]. The new preferred results, with the best accuracy and precision, are listed in the fourth column, along with their appropriate sources. The signs of nuclear magnetic moments (plus or minus) cannot be obtained from the usual NMR measurements. They were established using molecular beam magnetic resonance (the ABMR method), in which asymmetry in the absorption resonance curves upon introduction of an oscillating field can identify the quantum numbers and the sign of the nuclear moment. The spin quantum numbers with their parity are also included. Hydrogen isotopes were special because they have been known, to date, for their excellent accuracy and high precision. ^{1}H and ^{2}H isotopes can serve as good reference points, as they are found in many volatile hydride compounds (HD, HT, CH_4, NH_3, H_2O, CH_3F, SiH_4, PH_3, HCl) and as lock channels in the NMR apparatus. Therefore, it is possible to move ^{1}H or ^{2}H frequencies

doi:10.20944/preprints202512.0399.v1

and diamagnetic correction factors (shielding constants) to other nuclides using the list of molecules shown above (Table 1).

Table 2. Nuclear magnetic dipole moments of light nuclei.

Isotope	I(X)	$\mu(X)\mu_N$ Ref.[14]	$\mu(X)\mu_N$	Reference
^{1}H	1/2+	+2.792847351(9)	+2.79284734462(82)	Schneider *et al.*/2017 [15]
^{2}H	1+	+0.857438231(5)	+0.8574382335(22)	Puchalski *et al.*/2015 [16]
^{3}H	1/2+	+2.978962460(14)	+2.978962471(10)	Puchalski *et al.*/2015 [16]
^{3}He	1/2+	-2.12762531(3)	-2.1276253498(15)	Schneider *et al.*/2022 [17]
^{10}B	3+	+1.8004636(8)	+1.8004636(8)	Jackowski *et al.*/2009 [7]
^{11}B	3/2+	+2.688378(1)	+2.6883781(11)	Jackowski *et al.*/2009 [7]
^{13}C	1/2-	+0.702369(4)	+0.70236944(68)	Makulski *et al.*/2011 [18]
^{14}N	1+	+0.403573(2)	+0.40357368(7)	Makulski *et al.*/2022 [6]
^{15}N	1/2-	-0.2830569(14)	-0.28305791(3)	Makulski *et al.*/2022 [6]
^{17}O	5/2+	-1.893543(10)	-1.893553(2)	Makulski *et al.*/2018 [19]
^{19}F	1/2+	+2.628321(4)	+2.628335(11)	Jaszuński *et al.*/2012 [1]
^{21}Ne	3/2+	-0.66170(3)	-0.6617774(10)	Makulski *et al.*/2020 [20]
^{29}Si	1/2+	-0.555052(3)	-0.5550516(31)	Makulski *et al.*/2006 [21]
^{31}P	1/2+	+1.130925(5)	+1.1309246(50)	Lantto *et al.*/2011 [22]
^{33}S	3/2+	+0.64325(1)	+0.6432555(10)	Makulski/2022 [23]
^{35}Cl	3/2+	+0.82170(2)	+0.821721(5)	Jaszuński *et al.*/2013 [8]
^{37}Cl	3/2+	+0.68400(1)	+0.683997(4)	Jaszuński *et al.*/2013 [8]

Remember that the nuclear magnetic moments $\mu(X)\mu_N$ (written also as μ_X) shown in Table 2 are the projection value of the full vector onto the measurement axis. In fact the total length of the nuclear magnetic moment vector is $\mu_X^{\text{length}} = (\sqrt{(I_X(I_X+1)}/I_X)/\mu_X$ larger than this projection, despite this μ_X is commonly referred to in the literature as the nuclear magnetic moment. Sometimes, physicists make use of the g factor of nuclei instead of nuclear magnetic moments expressed in nuclear magnetons. The g factor (g value) is a dimensionless quantity which characterizes the magnetic properties of nuclei and can be ciphered as $g_X=\mu_X/\mu_N I_X$. For proton (^{1}H) g factor equals +2.79284734463(82)/1/2=+5.5856946893(16). On the other hand, the gyromagnetic ratio represented by the γ symbol, that describes the ratio of a nuclear magnetic moment to its angular momentum, is closely related to the following g factor: $\gamma_X=g\mu_N/\hbar$, where ħ is the h-bar. It can be expressed in SI units $s^{-1}T^{-1}$ or equivalently in $MHzT^{-1}$. The proton gyromagnetic ratio is $\gamma(^{1}H)$ is $2.6752218708(11)\cdot 10^{8}$ $s^{-1}T^{-1}$ or 42.577478461(18) MHz/T. The gyromagnetic ratio of a given nucleus plays an important role in both NMR and MRI spectroscopic methods. These three constants $\mu(X)$, $g(X)$ and $\gamma(X)$, which characterise the magnetic properties of nuclei are utilised alternatively in different branches of chemistry and physics. The appropriate analogs of nuclear moments one can find in Appendix 1.

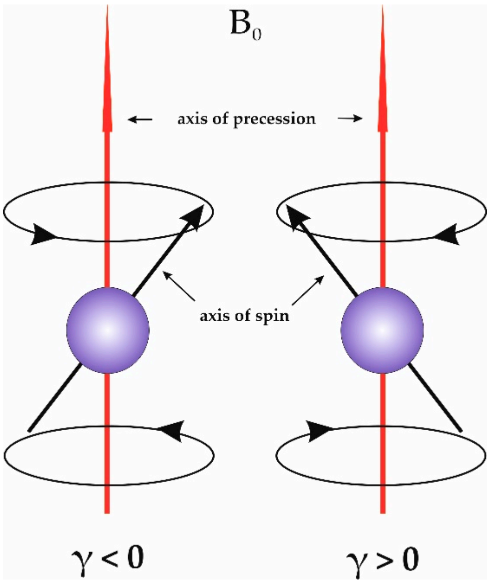

Figure 2. The sign of the gyromagnetic ratio γ is positive when the spin and nuclear magnetic moment are oriented in the same direction and negative when they are in opposite directions.

4. Discussion

The dipole magnetic moment of a proton (^{1}H) is a fundamental constant in nuclear physics, with far-reaching consequences for chemistry, physics, astrophysics, and quantum theory. It has been measured many times before. Recently, a direct, exact measurement was performed in the double Penning trap system by physicists at Mainz University [15]. The experiment was in two parts: the first step included isolation of a single proton in the magnetic trap, and the second step involved measurements of two frequencies – the spin-precession Larmor frequency and the cyclotron frequency of the proton in the magnetic field. Three individual protons were used, and the experiment lasted approximately 4 months, including preparatory work. The $\mu(^1H)$ result published in Science in 2017 was measured at 2.79284734463(82) μ_N, with an accuracy of 0.3 parts per billion. Deuteron (^{2}H/D) and triton (^{3}H/T) nuclear magnetic moments were determined from measurements of frequency ratios in HD and HT molecules, supplemented by precise calculations of the shielding effects of H, D, and T nuclei [16]. The shielding corrections of deuterium and tritium nuclei in HD and HT molecules are minimal, $\sigma(D)=26.372801(1)$ ppm (parts per million) and $\sigma(T)=26.391456(2)$ ppm. The operation of ^{3}H(T) is much more demanding because of its radioactivity. Triton has a long half-life of 12.32 years and can be taken as gaseous HT. The source of gaseous tritium gas (HT) can be titrated water (diluted HTO in excess of H_2O). Fortunately, tritium atoms decay by beta emission of low-energy electrons (average 5.7 keV), which can penetrate only 6 cm of air and cannot escape from NMR test tubes. Careful manipulation of samples is, despite everything, necessary.

Helium-3 was investigated in a Penning trap to directly measure the nuclear g-factor of the ^{3}He+ ion, shielded by only a single electron. The nuclear magnetic moment of the ^{3}He bare nucleus can be obtained by diamagnetic correction of 35.50738(3) ppm in He$^+$ ion [17]. The final result is $\mu(^3He)$ =-2.1276253498 (15) μ_N, with an accuracy of 0.7 parts per billion. The terrestrial ^{3}He gas can be supplied by some chemical trading companies (e.g., Chemgas, Isotec) at low pressures up to ~2.5 atm. It is beneficial that helium-3 can be mixed with appropriate gaseous substances and measured in conventional NMR spectrometers (see, for example: $^3He/H_2$, $^3He/NH_3$, ^{3}He/CO, and $^3He/CH_4$ and other mixtures) [23]. Analysis of these systems yields nuclear magnetic moments for ^{10}B, ^{11}B, ^{13}C, ^{14}N, ^{15}N, ^{31}P, and ^{33}S.

The ^{13}C nuclear magnetic moment was calculated in the enriched $^{13}CH_4$ molecule against ^{1}H parameters where $\nu_0(^{13}C)/\nu_0(^1H)$ is 0.2514473143(66) using shielding correction $\sigma_0(^{13}C)=195.02$ ppm. Confirmation of this result was achieved using helium-3 parameters, where $\nu_0(^{13}C)/\nu_0(^3He)$ in the

doi:10.20944/preprints202512.0399.v1

zero-pressure limit is 0.3300743617(61). The final results are in excellent agreement with each other. Analogously, the appropriate frequency ratios in the NH_3 molecule are as follows: $\nu_0(^{14}N)/\nu_0(^1H)$=0.0722342561(4) and $\nu_0(^{15}N)/\nu_0(^1H)$= 0.101327121(1). These numbers were corrected using new relativistic shielding constants for the nitrogen nucleus in ammonia, $\sigma_0(^{14/15}N)$=266.78 ppm. These last results of magnetic moments are confirmed using ^3He spectroscopic data. Similarly, accurate calculations were made in H_2O ($\sigma_0(^{17}O)$=328.4 ppm) and CH_3F ($\sigma_0(^{19}F)$=470.85 ppm) molecules to achieve ^{17}O [19] and ^{19}F [1] nuclear magnetic moments. ^{17}O-enriched water was dispersed in pure gases (Kr, Xe, CH_3F, and CF_3H), and ^1H and ^{17}O NMR spectra were recorded. The best calculations of magnetic shielding were performed in H_2O, the smallest oxygen-containing molecule suited for an NMR reference procedure. However, the ^1H and ^{19}F NMR spectra were measured in a pure CH_3F molecule.

In the case of the ^{29}Si nucleus, the stable silane, the silicon analog of methane, was employed [21]. The measured frequency ratio is $\nu_0(^{29}Si)/\nu_0(^1H)$= 0.198650063(1). The main error in the magnetic moment arises from the diamagnetic correction applied to the ^{29}Si shielding value. It can be as large as 2 ppm, depending on the precision of the theoretical calculations; $\sigma_0(^{29}SiH_4)$=482.85 ppm. Phosphine was the simplest phosphorus hydride compound used for gaseous experiments and NMR measurements of ^1H and ^{31}P NMR spectra. The glass samples containing ^3He/phosphine mixtures were prepared with great care due to PH_3's extremely poisonous, flammable, and explosive properties. The frequency ratios here are as follows: $\nu_0(^{31}P/\nu_0(^1H)$= 0.404698969 and $\nu_0(^{31}P)/\nu_0(^3He)$= 0.5312482456. The diamagnetic corrections were computed theoretically in absolute shielding units: $\sigma_0(^{31}P)$=614.758 ppm and $\sigma_0(^1H)$=29.305 ppm.

^{33}S is a quadrupolar nucleus and, consequently, its NMR signal widths are often large, depending on the chemical symmetry occupied by the nucleus in molecules. Short relaxation times in the gas phase also broadened signals for simple compounds such as SO_2, SO_3, H_2S, and CS_2. Fortunately, sulfur hexafluoride (SF_6) with a central sulfur atom bonded to six fluorine atoms has an octahedral geometry. SF_6 is a very stable gaseous substance. Several samples of gaseous $^3He/SF_6$ mixtures were prepared and analyzed by ^3He, ^{19}F, and ^{33}S NMR spectroscopy. The ratio of frequencies $\nu_0(^{33}S)/\nu_0(^3He)$= 0.10074480(17) were measured in the zero-pressure limit. The new nuclear magnetic moment of ^{33}S is in general agreement with previous results but is much more accurate. Recalculated shielding constant $\sigma_0(^{33}S)$ in the SF_6 molecule using Eq.(4) against ^{19}F parameters is 396.3 ppm in good agreement with $\sigma_0(^{33}S)$=392.6 ppm from theoretical calculations [23].

The last case of hydride compounds discussed here is hydrogen chloride, a gaseous substance in a mixture with helium-3, which was studied using ^1H, ^3He, ^{35}Cl, and ^{37}Cl NMR measurements [8]. The appropriate frequency ratios at the zero-pressure limit are as follows: $\nu_0(^{35}Cl)/\nu_0(^1H)$ = 0.0979818(4), $\nu_0(^{35}Cl)/\nu_0(^3He)$= 0.1286204(5), $\nu_0(^{37}Cl)/\nu_0(^1H)$ =0.0815596(9), and $\nu_0(^{37}Cl)/\nu_0(^3He)$= 0.1070630(1). The best ab initio calculations of shielding constants in an isolated HCl molecule give $\sigma_0(^{35/37}Cl)$=976.20 ppm and $\sigma_0(^1H)$=31.403 ppm. These were used to calculate $\mu(^{35}Cl)$ and $\mu(^{37}Cl)$ of bare nuclei.

Unfortunately, boron forms only one stable gaseous hydride, diborane (B_2H_6), which is very reactive with moisture and oxygen and highly toxic. We therefore decided to use fluorinated gas BF_3, which can be more safely handled and is commercially available [7]. A reference nucleus is now the ^{19}F nuclear magnetic moment. The experimental frequency ratios here are: $\nu_0(^{11}B)/\nu(^3He)$=0.42117005(4), $\nu_0(^{10}B)/\nu_0(^3He)$= 0.141033238(4), $\nu_0(^{11}B)/\nu_0(^{19}F)$=0.341028031(5), and $\nu_0(^{10}B)/\nu_0(^{19}F)$= 0.114196831(4). The diamagnetic corrections of boron nuclei are as follows: $\sigma(^{10}B)$=97.879 ppm and $\sigma(^{11}B)$=97.882 ppm, suggesting a small isotope effect. It is known that neon doesn't form stable compounds at normal conditions. Because of it, the ^{21}Ne moment was established from the ^1H moment and the frequency ratio $\nu(^{21}Ne)/\nu(^1H)$=0.07894287214(35) measured in gaseous neon against the proton resonance frequency of the residual signal of benzene-d_6 used in the lock system [20]. Diamagnetic correction applied for the neon nucleus in the neon atom is $\sigma(^{21}Ne)$=557.11 ppm.

The most abundant isotopes of argon, consisting of 18 protons and a different number of neutrons, are ^{40}Ar, ^{38}Ar, and ^{36}Ar. None of them possesses a magnetic moment and a non-zero spin number. In fact, argon is a unique case in the Periodic Table where contemporary NMR spectrometers have recorded no NMR spectra. However, spectroscopic measurements were carried out for ^{39}Ar nuclei [24], with nuclear spin I=7/2- and magnetic moment $\mu(^{39}\mathrm{Ar})=-1.590(5)\mu_N$, employing optical spectroscopy and a Fabry-Perrot interferometer with photoelectric detection. The ^{39}Ar nucleus is long-lived, with a half-life of 268(8) years; its samples are radioactive. They can be produced in the ^{39}K(n,p)^{39}Ar reaction. The quantity ratio of the ^{39}Ar/Ar was established as $\leq 4{\cdot}10^{-17}$. The nuclear magnetic moments of other short-lived argon isotopes were measured in fast-beam neutral-atom experiments, with reference to the NMR measurement of ^{37}Ar [25], and are presented in Ref.[26] with a few comments.

Interestingly, specific gas phase experiments were performed for heavy nuclei: ^{83}Kr (in gaseous krypton) [23,27], ^{129}Xe and ^{131}Xe (in gaseous xenon) [23,28], ^{183}W (for WF_6 in gaseous CF_4) [29], ^{117}Sn and ^{119}Sn (for $SnMe_4$ in gaseous CO_2 and N_2O) [30] and ^{207}Pb (for $PbMe_4$ in gaseous Xe and SF_6) [31]. Obviously, the NMR method can be applied to light and heavy nuclides, which are observed mainly in liquid solutions. Good examples are here: ^{6}Li and ^{7}Li (LiCl and $LiNO_3$ water solutions) [23,32–34], ^{23}Na (NaCl, $NaNO_3$, $NaClO_4$ water solutions) [23,35,36], ^{39}K (KCl and KNO_3 water solutions) [37], ^{77}Se ($SeMe_2$ molecule) [38], ^{79}Br and ^{81}Br (KBr · Kryptofix 222 complex) [39], ^{75}As (Na_3AsO_4) [40], ^{85}Rb and ^{87}Rb (RbCl and $RbNO_3$ water solutions) [41], ^{121}Sb, ^{123}Sb ($KSBF_6$) [40], ^{123}Te and ^{125}Te ($TeMe_2$ molecule)[38], ^{133}Cs (CsF, CsCl and $CsNO_3$ water solutions) [42] and finally ^{209}Bi ($Bi(NO_3)_3$ and $Bi(ClO_4)_3$ water solutions) [43,44]. Most of the papers listed above were published over the past ten years, underscoring the importance and status of nuclear magnetic moment investigations.

All experimental results mentioned above and preferred today are included in Table 2. The frequency ratios discussed above can be helpful for future recalculations if only better diamagnetic corrections become available. For convenience, the relevant nuclear magnetic moments $\mu(X)=h\gamma_X I_X=\mu_N g_X I_X$ in nuclear magnetons (μ_N) were recalculated to full-length analogs $\mu(X)^{length}$, g(X) factors, and gyromagnetic factors $\gamma(X)$, which can be found in Appendix A 1. The appropriate correction factors for $\mu(X)^{length}$ can be found in Appendix A2.

5. Conclusions

NMR experiments performed over the last 20 years in the gaseous state have been used to improve different nuclear magnetic moments with great success. Gases are well suited for this procedure because they allow the acquisition of NMR parameters for “isolated” molecules. Such molecules are not burdened by intermolecular interactions, which are relatively easily and accurately calculated using quantum-mechanical methods. Experimental frequencies can be obtained by measuring several gaseous samples at different pressures and extrapolating to the zero-pressure limit. For low-density gases, the use of enriched material is strongly recommended. This method is not limited to the gas phase but can, under certain conditions, be extended to liquids and solutions. Measurements of nuclear magnetic moments are among the most accurate in physics and chemistry. The precision of final results depends on the so-called “diamagnetic corrections,” which are more critical for heavier isotopes than for lighter ones. Therefore, theoretical advances in this field are crucial for establishing accurate nuclear magnetic moments. For the light nuclides discussed in this work, discrepancies between results (^{1}H–^{21}Ne) corrected using different shielding constants are usually below 0.0005%. In the case of ^{123}Sb, this error can be in the order of 0.01% of the magnetic moment and even higher for very heavy nuclei.

The best-known nuclear magnetic moment is that of the proton (^{1}H) nucleus, $+2.79284734463(82)\mu_N$. The analogous magnetic moment was estimated for the short-lived antiproton particle. Unique apparatus, the two-particle spectroscopy method in an advanced cryogenic multi-Penning trap system, employed at CERN, was also used for the measurement of the antiproton magnetic moment with a fractional precision of 1.5 ppb (parts per billion), showing that both magnetic moments of the proton and antiproton are practically equal [45]. The CPT (Charge Parity

Time) theorem is then satisfied, meaning that symmetry holds between particles and their antiparticles, which have identical masses, lifetimes, and magnetic moments. It is worth remembering that magnetic dipole moments are only one nuclear parameter among several others, such as size, shape, charge, electric quadrupole moment, and a few designated for unstable nuclei, such as decay mode and half-life. All of them serve as central points in the interpretation of nuclear structure building in physical theories of matter. The history of research on nuclear magnetic moments in the light of Gamow-Teller transitions was summarized [46], where several nuclear phenomena - configuration mixing, meson exchange currents, and relativistic effects are examined.

A universal, effective calculation method for predicting nuclear magnetic moments does not exist. Precise theoretical calculations of nuclear moments in light nuclei using the Lattice QCD (Quantum Chromodynamics) method are subject to several uncertainties due to lattice artifacts and contamination from excited states [47]. The best results show at least a slight discrepancy between theory and experiment. Contemporary progress in theoretical studies of nuclear magnetic moments can be found in Refs.[48,49]. We can say that modern chemical procedures play an essential role in the numerical establishment of nuclear moments [50], but benefits accrue exclusively to the nuclear physics, radiochemistry, and astrophysics sciences. Finally, currently available data indicate that nuclear magnetic moments are more experimental than theoretical, and even recently developed theoretical models remain approximate. Nevertheless, accurate nuclear magnetic moments can serve as good references for quantum-mechanical methods that provide the magnetic properties of particular nuclei. For specific cases of nuclei, we recommend an online-friendly database of nuclear electromagnetic moments available via a web browser [51]. Recently, N.J Stone published a short paper describing developments in the designation of nuclear magnetic and electric quadrupole moments not only of stable nuclei but also in short-lived states (<1ms) [52]. In summary, he noted that over the past thirty years, interest in the subject referred to in the title of this paper (“Nuclear moments: recent developments”) is still great and continuous. We refer the reader to this interesting publication.

Funding: This research received no external funding.

Data Availability Statement: The original contributions presented in this study are included in the article. Further inquiries can be directed to the corresponding authors.

Conflicts of Interest: The authors declare no conflicts of interest.

Abbreviations

The following abbreviations are used in this manuscript:

NMR	Nuclear Magnetic Resonance
NMM	Nuclear Magnetic Moment

Appendix A

Table A1. Different values of magnetic properties for light nuclei from ^{1}H up to ^{37}Cl.

Isotope	$\mu^{\text{length}}/\mu_N$	g_X	$\gamma(X)\times10^7$ $s^{-1}T^{-1}$	$\gamma(X)/2\pi$ $MHzT^{-1}$
^{1}H	+4.837353498(1)	+5.585694689(2)	+26.752218759(8)	42.57747854(1)
^{2}H	+1.212600779(3)	+0.857438234(2)	+4.10662889(1)	6.53590288(2)
^{3}H	+5.159714352(2)	+5.95792494(2)	+28.53498451(1)	45.4148384(2)
^{3}He	+3.685155205(3)	+4.255250700(3)	+20.38016826(1)	+32.43604519(2)
^{10}B	+2.0789963(9)	+0.6001545(3)	+2.8743899(1)	+4.574734(2)
^{11}B	+3.470681(1)	+1.7922521(7)	+8.583842(4)	+13.661609(6)
^{13}C	+1.216540(1)	+1.404739(1)	+6.727879(7)	+10.70775(1)
^{14}N	+0.5707394(1)	+0.40357368(7)	+1.9328824(3)	+3.076278(1)
^{15}N	-0.49027068(5)	-0.56611582(6)	-2.711364(3)	-4.3152706(5)

^{17}O	-2.240482(2)	-0.7574212(8)	-3.627605(4)	-5.773512(6)
^{19}F	+4.55241(2)	+5.25667(2)	+25.1764(1)	+40.0695(2)
^{21}Ne	-0.854351(1)	-0.4411849(7)	-2.113018(3)	-3.362973(5)
^{29}Si	-0.961378(2)	-1.110103(2)	-5.31675(1)	-8.46187(2)
^{31}P	+1.958819(8)	+2.26185(1)	+10.83294(5)	+17.241156(8)
^{33}S	+0.830439(2)	+0.428837(1)	+2.053879(3)	+0.32688500(5)
^{35}Cl	+1.060837(7)	+0.547814(3)	+2.62371(2)	+4.17576(3)
^{37}Cl	+0.883036(5)	+0.455998(3)	+2.18396(1)	+3.47589(2)

Table A2. Multipliers for the calculation of full length for the nuclear magnetic vector used in Appendix A1.

I_X	Nucleus example	$\sqrt{(I_X(I_X + 1)}/I_X$
1/2	^{1}H,^{3}H,^{3}He,^{13}C,^{15}N,^{19}F,^{29}Si,^{31}P	1.7320508076
1	^{2}H,^{14}N	1.4142135624
3/2	^{11}B,^{21}Ne,^{33}S,^{35}Cl,^{37}Cl	1.2909944487
2	^{204}Tl	1.2247448714
5/2	^{17}O	1.1832159566
3	^{10}B	1.1547005384
7/2	^{39}Ar,^{45}Sc,^{49}Ti,^{51}V	1.1338934190
4	^{40}K	1.1180339887
9/2	^{73}Ge,^{83}Kr	1.1055415968

References

1. Jaszuński M., Antušek A., Garbacz P., Jackowski K., Makulski W., Wilczek M., The determination of accurate nuclear magnetic dipole moments and direct measurement of NMR shielding constants, *Prog. Nucl. Magn. Reson. Spectrosc.*, **2012**, *67*, 49-63. DOI:10.1016/j.pnmrs.2012.03.002
2. Antušek A., Jackowski K., Jaszuński M., Makulski W., Wilczek M., Nuclear magnetic dipole moments from NMR spectra, *Chem. Phys. Lett.*, **2005**, *411*, 111-116. https://doi.org/10.1016/j.cplett.2005.06.022
3. Jackowski K., Wilczek M., Measurements of Nuclear Magnetic Shielding in Molecules, *Molecules*, **2024**, *29*, 2617. https://doi.org/10.3390/molecules29112617
4. Antušek A., Jaszuński M., Accurate Nonrelativistic Calculations of NMR Shielding Constants, in Gas Phase NMR, Eds.: Jackowski K. & Jaszuński M., RSC., London, § 6., 2016. pp. 186-217. Doi: https://doi.org/10.1039/9781782623816-00186
5. Makulski W., Deuterium isotope effects on ^{17}O nuclear shielding in a single water molecule from NMR gas phase measurements", *Phys. Chem. Chem. Phys.*, **2020**, *22*, 17777-17780. DOI: 10.1039/d0cp03085f
6. Makulski W., Aucar J.J., Aucar G.A., Ammonia: the molecule for establishing ^{14}N and ^{15}N absolute shielding scales and a source of information on nuclear magnetic moments, *J. Chem. Phys.* **2020**, 157(8), 084306. https://doi.org/10.1063/5.0096523
7. Jackowski K., Makulski W., Szyprowska A., Antušek A., Jaszuński M., Jusélius J., NMR shielding constants in BF_3 and magnetic dipole moments of ^{10}B and ^{11}B nuclei, *J. Chem. Phys.*, **2009**, *130*, 044309. https://doi.org/10.1063/1.3065670
8. Jaszuński M., Repisky M., Demissie T.B., Komorovsky S., Malkin E., Ruud K., Garbacz P., Jackowski K., Makulski W., Spin-rotation and NMR shielding constants in HCl, *J. Chem. Phys.*, **2013**, *139*, 234302-1-6. https://doi.org/10.1063/1.4840295
9. Garbacz P., Jackowski K., Makulski W., Wasylishen R.E., Nuclear Magnetic Shielding for Hydrogen in Selected Isolated Molecules, *J. Phys. Chem.A*, **2012**, *116*, 11896. DOI: 10.1021/jp309820v
10. Makulski W., Absolute ^{13}C Nuclear Magnetic Shielding of Simple Isolated Molecules from Gas Phase Measurements, *Phys. Chem. Chem. Phys.*, **2022**, *24*, 8950-8961. https://doi.org/10.1039/D2CP00231K
11. Jameson C.J., Fundamental Intramolecular and Intermolecular Information from NMR in Gas Phase, Eds.: Jackowski K.& Jaszuński M., RSC., London, § 1, 2016, pp.1-51. Doi: https://doi.org/10.1039/9781782623816-00001

12. Bajac D.F.E., Aucar I.A., Aucar G.A., Absolute NMR shielding scales in methyl halides obtained from experimental and calculated nuclear spin-rotation constants, *Phys. Rev. A*, **2021**, *104*, 012805. DOI: https://doi.org/10.1103/PhysRevA.104.012805
13. Aucar G.A., Aucar I.A., Recent Developments in Absolute Shielding Scales for NMR Spectroscopy, *Annu. Rep. NMR Spectrosc*., 96 (2019) pp. 77-141. DOI: 10.1016/bs.arnmr.2018.08.001
14. Stone N.J., Table of Recommended Nuclear Magnetic Dipole Moments: Part 1, Long-Lived States, INDC International Nuclear Data Committee, Vienna International Centre, P.O. Box 100, 1400 Vienna, Austria. https://nds.iaea.org/publications/indc/indc-nds-0794.pdf
15. Schneider G., Mooser A., Bohman M., Schön N., Harrington J., Higuchi T., Nagahama H., Sellner S., Smorra C., Blaum K., Matsuda Y., Quint W., Walz J., Ulmer S., Double-trap measurement of the proton magnetic moment at 0.3 parts per billion precision. *Science*, **2017**, *358* (6366), 1081-1084. DOI: 10.1126/science.aan0207
16. Puchalski M., Komasa J., Spyszkiewicz A., Pachucki K., Nuclear magnetic shielding in HD and HT, *Phys. Rev.A*, **2022**, *105*, 042802. DOI: 10.1103/PhysRevA.105.042802
17. Schneider A., Sikora B., Dickopf S., Müller M., Oreshkina N.S., Rischka A., Valuev I.A., Ulmer S., Walz J., Harman Z., Keitel C.H., Mooser A., Blaum K., Direct measurement of the $^{3}He^{+}$ magnetic moments, *Nature*, **2022**, *606*, 878–883. https://doi.org/10.1038/s41586-022-04761-7
18. Makulski W., Szyprowska A., Jackowski K., Precise determination of the ^{13}C nuclear magnetic moment from ^{13}C, ^{3}He and ^{1}H NMR measurements in the gas phase, *Chem. Phys. Lett*. **2011**, *511*, 224–228. DOI:10.1016/j.cplett.2011.06.065
19. Makulski W., Wilczek M., Jackowski K., ^{17}O and ^{1}H NMR spectral parameters in isolated water molecules, *Phys. Chem. Chem. Phys*., **2018**, *20*, 22468. DOI: 10.1039/c8cp01748d
20. Makulski W., Garbacz P., Gas-phase ^{21}Ne NMR studies and the nuclear magnetic dipole moment of neon-21, *Magn. Reson. Chem*., **2020**, *58*, 648-652. https://doi.org/10.1002/mrc.5006
21. Makulski W., Jackowski K., Antušek A., Jaszuński M., Gas-phase NMR measurements, absolute shielding scales and magnetic dipole moments of ^{29}Si and ^{73}Ge nuclei, *J. Phys. Chem.A*., **2006**, *110*, 11462.
22. Lantto P., Jackowski K., Makulski W., Olejniczak M., Jaszuński M., NMR shielding constants in PH_3, absolute shielding scale and the nuclear magnetic moment of ^{31}P , *J. Phys. Chem.A*, **2011**, *115*, 10617. DOI: 10.1021/jp2052739
23. Makulski W., Probing nuclear dipole moments and magnetic shielding constants through 3-helium NMR spectroscopy, Physchem. (MDPI) 2(2) (2022) 116-130. https://doi.org/10.3390/physchem2020009
24. Traub W., Roesler F.L., Robertson M.M., Cohen V.W., Spectroscopic Measurement of the Nuclear Spin and Magnetic Moment of ^{39}Ar, *J. Opt. Soc. Am*., **1967**, *57(12)*, pp. 1452-1458. https://doi.org/10.1364/JOSA.57.001452
25. Klein A., Brown B.A., Georg U., Keim M., Lievens P., Neugart R., Neuroth M., Silverans R.E., Vermeeren L., ISOLDE Collaboration, Moments and mean square charge radii of short-lived argon isotopes, *Nucl. Phys.A*, **1996**, 602, 1-22. https://doi.org/10.1016/0375-9474(96)00192-3
26. Makulski W., Explorations of Magnetic Properties of Noble Gases: the Past, Present and Future, *Magnetochemistry*, **2020**, 6(4), 46. https://doi.org/10.3390/magnetochemistry6040065
27. Makulski W., ^{83}Kr nuclear magnetic moment in terms of that of ^{3}He, *Magn. Reson. Chem*., **2014**, *52*, 430-434. https://doi.org/10.1002/mrc.4083
28. Makulski W., ^{129}Xe and ^{131}Xe Nuclear Magnetic Dipole Moments from Gas Phase NMR Spectra, *Magn. Reson. Chem*., **2015**, *53*, 273-279. DOI: 10.1002/mrc.4191
29. Garbacz P., Makulski W., ^{183}W nuclear dipole moment determined by gas-phase NMR spectroscopy, *Chem. Phys*., **2017**, *498-499*, 7-11. https://doi.org/10.1016/j.chemphys.2017.10.00
30. Makulski W., Tetramethyltin study by NMR Spectroscopy in the gas and liquid phase, *J. Mol. Struct*., **2012**, *1017*, 45. https://doi.org/10.1016/j.molstruc.2012.02.072
31. Adrian B., Makulski W., Jackowski K., Demissie T.B., Ruud K., Antušek A., Jaszuński M., NMR shielding scale and the nuclear magnetic dipole moment of ^{207}Pb, *Phys. Chem. Chem. Phys*., **2016**, *18*, 16483-90. DOI: 10.1039/c6cp01781a

32. Makulski W., The Radiofrequency NMR Spectra of Lithium Salts in Water; Reevaluation of Nuclear Magnetic Moments for ^{6}Li and ^{7}Li, *Magnetochemistry*, **2018**, *4*, 9. https://doi.org/10.3390/magnetochemistry4010009
33. Pachucki K., Patkóš V., Yerokhin V.A., Accurate determination of ^{6,7}Li nuclear magnetic moments, *Phys. Lett.B*, **2023**, *846*, 138189, https://doi.org/10.1016/j.physletb.2023.138189
34. Neronov Yu.I. Determination of the magnetic moments of ^{6}Li and ^{7}Li nuclei using an NMR spectrometer that records signals from two nuclei simultaneously. *Izmeritel`naya Tekhnika*. **2020**, *9*, 3-8. (In Russ.) https://doi.org/10.32446/0368-1025it.2020-9-3-8
35. Makulski W., Multinuclear Magnetic Resonance Study of Sodium Salts in Water Solutions, *Magnetochemistry*, **2019**, *5*, 68. https://doi.org/10.3390/magnetochemistry5040068
36. Yu. I. Neronov Yu. I., Determination of the Magnetic Moment of a 23Na Nucleus Using an NMR Spectrometer with Simultaneous Detection of Signals from Two Nuclei, Technical Physics, **2021**, *66(1)* 93-97. DOI: 10.1134/S106378422101014X
37. Neronov Yu. I., Pronin A. N., Study of Nuclear Magnetic Resonance Spectra of Potassium Ions in Aqueous Solutions and Estimation of the Magnetic Moment of the ^{39}K Nucleus, *Measurement Techniques*, **2021**, *64(6)*, 267–272. https://doi.org/10.1007/s11018-021-01928-y
38. Hurajt A., Antušek A., NMR shielding constants and rederivation of accurate magnetic dipole moments of ^{77}Se, ^{123}Te, and ^{125}Te nuclei, *J. Chem. Phys*. **2025**, *163*, 144306. https://doi.org/10.1063/5.0287373
39. Gryff-Keller A., Molchanov S., Wodyński A., Scalar relaxation of the second kind - a potential source of information on the dynamics of molecular movements. 2. Magnetic dipole moments and magnetic shielding of bromine nuclei. *J Phys Chem.A*., **2014**, *118(1)*, 128-33. doi: 10.1021/jp410160c.
40. Hurajt A., Kędziera D., Kaczmarek-Kędziera A., Antušek A., Nuclear magnetic dipole moments of ^{75}As, ^{121}Sb, and ^{123}Sb from ab initio calculations of NMR shielding constants and existing NMR experiments, *Phys. Rev.A*, **2024**, *109*, 042815. DOI: 10.1103/PhysRevA.109.042815
41. Neronov Yu. I., Pronin A.N., Study of NMR Signals of Rubidium in Aqueous Solutions and Determination of the Magnetic Moments of Rb-85 and Rb-87 Nuclei, Technical Physics, **2024**, *68(S3)*, S478-S484. DOI: 10.1134/S106378422390070X
42. Neronov, Yu. I., Pronin, A. N., NMR Spectra of Cesium in Aqueous Solutions. Determination of the Magnetic Moment of Cesium-133 Nucleus, *Measurement Techniques*, **2022**, *64(11)* 865-870. https://doi.org/10.1007/s11018-022-02016-5
43. Antušek A., Jaszuński M., Misiak M., Makulski W., Jackowski K., Nuclear magnetic dipole moment of ^{209}Bi from NMR experiments, *Phys. Rev. A*., **2018**, *98*, 052509. DOI: https://doi.org/10.1103/PhysRevA.98.052509
44. Skripnikov L.V., Schmidt S., Ullmann J., Geppert C., Kraus F., Kresse B., Nörtershäuser W., Privalov A.F., Scheibe B., Shabaev V.M., Vogel M., Volotka A.V., New Nuclear Magnetic Moment of ^{209}Bi: Resolving the Bismuth Hyperfine Puzzle, *Phys. Rev. Lett*., **2018**, *120(9)*, 093001. doi:10.1103/PhysRevLett.120.093001
45. Smorra C., Sellner S., Borchert M.J., Harrington J.A., Higuchi T., Nagahama H., Tanaka T., Mooser A., Schneider G., Bohman M., Blaum K., Matsuda Y., Ospelkaus C., Quint W., Walz J., Yamazaki Y., Ulmer S., A parts-per-billion measurement of the antiproton magnetic moment, *Nature*, **2017**, *550*, 371–374. https://doi.org/10.1038/nature24048
46. Arima A., A short history of nuclear magnetic moments and GT transitions, *Sci. China Phys. Mech. Astron*., **2011**, *54*, 188–193. https://doi.org/10.1007/s11433-010-4224-6
47. Wang T., Lattice Calculation of Nuclear Magnetic Dipole Moment. https://indico.ihep.ac.cn/event/24637/attachments/88211/113819/Dipole%20Moment.pdf
48. Zhao E., Recent progress in theoretical studies of nuclear magnetic moments, *Chin. Sci. Bull*., **2012**, *57(34)*. DOI:10.1007/s11434-012-5491-6
49. Li J., Meng J., Nuclear magnetic moments in covariant density functional theory, *Front. Phys*. **2018**, *13*, 132109. https://doi.org/10.1007/s11467-018-0842-7
50. Castel B., Towner I.S., Modern Theories of Nuclear Moments, (1990) Oxford, 1990; online edn, Oxford Academic, 31 Oct. 2023), https://doi.org/10.1093/oso/9780198517283.001.0001, accessed 18 Oct. 2025

51. T.J. Mertzimekis, An online database of nuclear electromagnetic moments, *Phys. Res.* A, **2016**, *807*, 56-60. DOI: 10.1016/j.nima.2015.10.096
52. Stone N.J., Nuclear moments: recent developments, *Interactions*, **2024**, *245*, 50. https://doi.org/10.1007/s10751-024-01896-z.